HHS Public Access

Author manuscript

FASEB J. Author manuscript; available in PMC 2024 March 05.

Published in final edited form as:

FASEB J. 2023 December ; 37(12): e23316. doi:10.1096/fj.202301722R.

Lactate produced by alveolar type II cells suppresses inflammatory alveolar macrophages in acute lung injury

René M. Roy[1], **Ayed Allawzi**[2,3], **Nana Burns**[2,3], **Christina Sul**[2,3], **Victoria Rubio**[1,2], **Jessica Graham**[1], **Kurt Stenmark**[2,3], **Eva S. Nozik**[2,3], **Rubin M. Tuder**[3,4], **Christine U. Vohwinkel**[2,3]

[1]Children's Hospital Colorado, University of Colorado, Anschutz Medical Campus, Aurora, Colorado, USA

[2]Division of Pediatric Critical Care, Department of Medicine, University of Colorado, Anschutz Medical Campus, Aurora, Colorado, USA

[3]Developmental Lung Biology, Cardiovascular Pulmonary Research Laboratories, University of Colorado, Anschutz Medical Campus, Aurora, Colorado, USA

[4]Division of Pulmonary Sciences and Critical Care Medicine, Program in Translational Lung Research, University of Colorado School of Medicine, Aurora, Colorado, USA

Abstract

Alveolar inflammation is a hallmark of acute lung injury (ALI), and its clinical correlate is acute respiratory distress syndrome—and it is as a result of interactions between alveolar type II cells (ATII) and alveolar macrophages (AM). In the setting of acute injury, the microenvironment of the intra-alveolar space is determined in part by metabolites and cytokines and is known to shape the AM phenotype. In response to ALI, increased glycolysis is observed in AT II cells, mediated by the transcription factor hypoxia-inducible factor (HIF) 1α, which has been shown to decrease inflammation. We hypothesized that in acute lung injury, lactate, the end product of glycolysis, produced by ATII cells shifts AMs toward an anti-inflammatory phenotype, thus mitigating ALI. We found that local intratracheal delivery of lactate improved ALI in two different mouse models. Lactate shifted cytokine expression of murine AMs toward increased IL-10, while decreasing *IL-1* and *IL-6* expression. Mice with ATII-specific deletion of *Hif1a* and mice treated with an inhibitor of lactate dehydrogenase displayed exacerbated ALI and increased inflammation with decreased levels of lactate in the bronchoalveolar lavage fluid; however, all those parameters improved with intratracheal lactate. When exposed to LPS (to recapitulate an inflammatory stimulus as it occurs

Correspondence: Christine U. Vohwinkel, Developmental Lung Biology, Cardiovascular Pulmonary Research Laboratories, University of Colorado, Anschutz Medical Campus, Aurora, CO, USA. christine.vohwinkel@cuanschutz.edu.
René M. Roy and Ayed Allawzi contributed equally.

AUTHOR CONTRIBUTIONS

Christine U. Vohwinkel, René M. Roy, Ayed Allawzi, Eva S. Nozik, and Rubin M. Tuder designed the research studies. Christine U. Vohwinkel, René M. Roy, Victoria Rubio, Ayed Allawzi, Jessica Graham, Christina Sul, and Nana Burns conducted the experiments. Christine U. Vohwinkel, Ayed Allawzi, Christina Sul, and René M. Roy analyzed the data. Christine U. Vohwinkel, Ayed Allawzi, and René M. Roy wrote the manuscript and provided all figures. Rubin M. Tuder, Eva S. Nozik, and Kurt Stenmark revised the manuscript.

DISCLOSURES

The authors declare no conflicts of interest.

SUPPORTING INFORMATION

Additional supporting information can be found online in the Supporting Information section at the end of this article.

in ALI), human primary AMs co-cultured with alveolar epithelial cells had reduced inflammatory responses. Taken together, these studies reveal an innate protective pathway, in which lactate produced by ATII cells shifts AMs toward an anti-inflammatory phenotype and dampens excessive inflammation in ALI.

Keywords

acute lung injury; acute respiratory distress syndrome; alveolar epithelium; alveolar macrophage; glycolysis; hypoxia-inducible factor; lactate

1 | INTRODUCTION

Inflammation is a hallmark of acute lung injury (ALI) and its clinical manifestation, acute respiratory distress syndrome (ARDS), which carries a significant disease burden both regarding morbidity and mortality.[1] Our previous work showed that in response to injury, alveolar epithelial type II cells (ATII) demonstrate enhanced glycolysis via the hypoxia-inducible factor (HIF)-1A-phosphofructokinase-2/fructose-2,6-bisphosphatase (PFKFB) 3 axis, which was associated with attenuation of inflammation in the acute phase of acute lung injury in several models of murine ALI.[2–4] Alveolar macrophages (AMs) reside in the alveolar space near ATII cells[5] and in this niche, the phenotype of the AMs is affected by the local microenvironment consisting of metabolites, cytokines, and surrounding cells that shape their inflammatory or anti-inflammatory properties.[6] The critical role of alveolar macrophages (AM) in the pathogenesis of ALI/ARDS, especially in the inflammatory phase, has been well-established in animal models and human disease.[7,8] In the present work, we focus on the interaction between alveolar type II cells and AM, with particular emphasis on how ATII cells can shape the metabolic microenvironment and therefore potentially suppress the inflammatory phenotype of AM in ALI. It has been shown that macrophages can reversibly change their activation state depending on their environment.[6,9] Alterations in the metabolic microenvironment can shape the inflammatory phenotype of macrophages, as demonstrated in tumor-associated macrophages—as lactate, derived from tumor cells, can shift the surrounding macrophages toward a VEGF and ARG-1-expressing pro-resolving phenotype[10]; however, it is unknown whether AMs, key regulators of pathogenesis in ALI/ARDS and substantially different from tumor-associated macrophages, respond to lactate in a similar fashion. We hypothesized that lactate derived from ATII cells and released into the intra-alveolar microenvironments can mitigate the inflammatory phenotype of AMs and serve as an endogenous protective pathway that quenches excessive alveolar inflammation in ALI.

2 | METHODS

2.1 | Materials

Unless otherwise noted, chemicals were obtained from Sigma (St. Louis/MO, USA). FX-11 (CAS No.: 213971–34–7) was obtained from Millipore Corp Billerica/MA, USA.

2.2 | Ethics statement

2.2.1 | Mice—The local institutional animal care and use committee (University of Colorado, Anschutz Medical Campus) approved all animal experiments (protocol numbers B104914(06)1D B104917(04)E and 00128). Animal experiments were carried out in accordance with the US Law on the Protection of Animals and the National Institutes of Health guidelines for the use of live animals.

2.2.2 | Humans—Human airway macrophages were obtained from BALF from lungs rejected for transplantation as previously described[11] through a collaboration with the National Jewish Hospital (Denver/CO, USA). The Colorado Multiple Institutions Review Board approved all human protocols and waived the requirement for informed consent for the use of de-identified BALF samples.

2.3 | Mice

Wild-type mice (C57BL/6J) were purchased from Jackson laboratories (#000664 C57BL/6J, RRID:IMSR_ JAX:000664). Mice with the Cre-Lox recomination system exclusively expressed in alveolar type 2 cells SPC-ER-Cre+ ($Sftpc^{tm1(cre/ERT2)Blh}$), JAX stock #028054 (IMSR Cat# JAX:028054, RRID:IMSR_JAX:028054) were generously provided by from Bridget Hogan (Duke University, Durham/NC, USA).[12] To generate mice with AT II-specific *Hif1a* deletion, $Hif1a^{loxp/loxp}$ (RRID:IMSR_JAX:007561) mice were crossed with the SPC ER Cre animals. $Hif1a^{loxp/loxp}$ SPC-ER-Cre+ were previously described.[3,4] Conditional knockout was induced by 75 mg/kg/d i.p tamoxifen (Sigma-Aldrich) over 5 days as described,[13] with control animals also receiving tamoxifen. Genotyping PCR performed on tails was used to determine Cre and loxp expression as well as Cre-flox expression (GeneTyper, New York/NY, USA). SPC-ER Cre animals were used as controls for the $Hif1a^{loxp/loxp}$ SPC-ER-Cre+ animals. Male and female mice between 8 and 12 weeks of age, weighing 18–25 g, at the time of harvest were used for all genotypes. Experiments were conducted on weight, sex, and age-matched animals. All animals were housed under a 12-h light/12-h dark cycle.

2.4 | Murine models of acute lung injury

We utilized intratracheal administration of hydrochloric acid to simulate aspiration of acidic gastric contents or LPS to induce direct ALI.

2.4.1 | Acid aspiration-induced lung injury—The acid aspiration model of ALI was described previously.[3,4,14,15] Mice were anesthetized with isoflurane and suspended by their incisors at 45° angle. Fifty-microliter of 0.125 M hydrochloric acid (HCl) was instilled intratracheally. Control animals received 50 μL of 0.9 M NaCl, which was pH controlled to the pH of hydrochloric acid.

2.4.2 | LPS-induced lung injury—Age- (8–12 weeks old) and sex-matched mice were anesthetized with pentobarbital (70 mg/kg) and LPS (*Escherichia coli* 0111:B4, L4391; Sigma, St. Louis, MO, USA (5 μg/g body weight) was administered intratracheally via a 22-gauge catheter.

2.4.3 | Intratracheal instillation of lactate—After the induction of ALI (6 h), mice received 50 μL 25 mM lactate solution. To control for the potential effect of lactic acid reduction in pH (pH range of 25 mM lactate solution was 7.10–7.15), the respective control group received an equal volume of pH-matched PBS to control for the potential effect of lactic acid reduction in pH.

2.5 | Isolation of murine alveolar type 2 cells

Primary alveolar epithelial type II cells (AT II) were isolated from mice as described previously.[4,16,17] Briefly, mice were anesthetized intraperitoneally with 70 mg/kg pentobarbital and exsanguinated by removing the left atrium. Lungs were then perfused with sterile PBS via the right ventricle. Dispase (Corning) was then instilled intratracheally followed by a low-melting point agarose plug. Lungs were removed intact and incubated for 45 min at room temperature. Tissue was teased apart manually and then passed through a 70-micron cell strainer (BD Bioscience, Franklin Lakes/NJ, USA). The cell mixture was then labeled with a mixture of biotinylated antibodies against CD16/32, TER119, CD 45, and CD90 (all from BD Bioscience, Franklin Lakes/NJ, USA: BD Biosciences Cat# 553143, RRID:AB_394658, BD Biosciences Cat# 553672, RRID:AB_394985, BD Biosciences Cat# 553078, RRID:AB_394608, and BD Biosciences Cat# 554896, RRID:AB_395587), and subsequently incubated with streptavidin-labeled magnetic beads (Promega Corporation, Madison/WI, USA) for negative selection for AT II cells. In the final step, fibroblasts were removed by adhering to a Petri dish for 2 h. AT II cells were cultured as described previously[18,19] in DMEM with 4.5 g/L glucose and stable L-glutamine, 10% fetal bovine serum (FBS-LOT 27021001), and 1% penicillin/streptomycin mix (all from Corning Cellgro, Manassas/VA, USA). Cells were incubated in a humidified atmosphere of 5% CO_2/95% air at 37°C.

2.6 | Isolation of bone marrow-derived macrophages

Mice were euthanized with pentobarbital and bone marrow was flashed from femur and tibia into a 50 mL conical tube with ice-cold PBS and then centrifuged. Cells were resuspended in 100 mL DMEM 4.5 g/L glucose, pyruvate, and HEPES media (Corning), supplemented with 20 ng/mL M-CSF-1 (R&D Systems, Minneapolis/MN USA) and 10% FBS (Thermo Fisher, Waltham/MA USA). The cell suspension was transferred to a T-150 (Thermo Fisher) flask and incubated for 3 days prior to replating for specific experiments.

2.7 | Primary human alveolar macrophages

AMs obtained from lungs rejected for transplant were isolated by bronchoalveolar lavage (BAL) of the right middle lobe by filling the lobe three times with a balanced salt solution and EDTA, and then three times with the salt solution alone. After each installation, the aspirated fluid was collected, pooled, and centrifuged.

2.8 | Macrophage and alveolar epithelial cell co-culture system

Co-culture experiments were conducted according to.[20,21] Briefly, for co-culture experiments, 2.5×10^5 A549 cells (ATCC Cat# CRM-CCL-185, RRID:CVCL_0023) or 5×10^5 AT II cells per well were seeded on the bottom side of transwell plates (from

Costar/Corning) and after 2 days subsequently co-cultured with BMDMs or primary human macrophages (density 2.5×10^5 cells/well), that were seeded on the apical side of the transwell insert medium utilized was DMEM with 4.5 g/L glucose and stable L-glutamine, 10% fetal bovine serum (FBS), 1% penicillin/streptomycin mix (all from Corning Cellgro, Manassas/VA, USA), and amphotericin B (250 μg/mL). Cells were incubated in a humidified atmosphere of 5% CO_2 at 37°C.

2.9 | Supernatant preparation and collection

AT II cells were grown in DMEM plus supplements. Fractionation of cell culture supernatants was achieved using Amicon Ultra centrifugal filters (3K Ultracel, Millipore Burlington/MA, USA). The supernatant fraction >3 kDa remained above the filter, and the fraction <3 kDa passed through to the lower chamber.

2.10 | Determination of lactate concentration

The L-lactate concentration in BALF was measured using a Lactate Assay Kit (Sigma Aldrich) according to the manufacturer's instructions.

2.11 | Sample collection

At the experimental endpoint with mice under deep anesthesia, lungs were lavaged three times with 1 mL of PBS per passage to obtain bronchoalveolar lavage fluid. Retrieved lavage fluid was at 300 g for 5 min at 4°C and resulting cell-free BAL was immediately snap-frozen for subsequent measurement of protein and ELISA studies. For pulmonary tissues, the lungs were flushed with 10 mL saline via the right ventricle, and either snap-frozen in liquid nitrogen and stored at −80°C or conserved in formalin for histologic analysis.

2.12 | Histopathological evaluation of acute lung injury

Lungs were explanted and prepared for paraffin embedding as described.[14] Five micrometer sections were stained with H&E. Assessment of histological lung injury was performed by grading as follows[22]: infiltration or aggregation of inflammatory cells in air space or vessel wall: 1, only wall; 2, few cells (one to five cells) in air space; 3, intermediate; 4, severe (air space congested); interstitial congestion and hyaline membrane formation: 1, normal lung; 2, moderate (<25% of lung section); 3, intermediate (25%–50% of lung section); 4, severe (>50% of lung section); and hemorrhage: 0, absent; 1, present. Six representative images were obtained from each animal and were analyzed by two investigators blinded to group assignments.

2.13 | Measurement of BALF protein content

The protein content of BALF was measured via Bradford assay as described previously.[23]

2.14 | Tissue digest

To prepare cell suspension for downstream flow cytometry experiments, lungs were processed as previously described.[19] In brief, lungs were isolated and digested in Liberase TM and DNAse (MilliporeSigma) at a final concentration of 0.4 mg/mL and 100 U,

respectively. Lungs were then further processed mechanically using the GentleMACS System using the preinstalled program m_lung_01_02, incubated for 25 min at 37°C, and then dissociated again using the program m_lung_02 for 8 s. The digestion was terminated by adding FBS to a final concentration of 20%. Cell suspension was then filtered through a 70-μm mesh and spun for 10 min at 300 *g*, followed by red blood cell lysis (Thermo Fisher Scientific) according to the manufacturer's guidelines. Cells were then passed through a 40-μm mesh to prevent clumps from forming and pelleted for downstream processing.

2.15 | Flow cytometry

Flow cytometry experiments were conducted as previously described.[24] Briefly, buffer consisting of PBS, 1 mM EDTA, 10 mM HEPES, pH 7.3, and 1% FBS was used throughout all washing and incubation steps. Flow cytometry analysis was performed on Gallios 561 nm (Beckman Coulter) and Yeti (Propel Labs, Fort Collins, CO, USA) devices. The sorting strategy excluded debris and cell doublets using light scatter (forward and side scatter), whereas dead cells were excluded by DAPI-positive staining (1 μg/mL). Fluorescence-Minus One controls were used to determine gating areas. Monocytes, neutrophils, B cells, and T cells were excluded in the $Dump^+$ gate. $Dump^-$ gate was then selected, and $CD45^+$ population was then segregated into recruited AMs ($Dump^-$, $CD45^+$, $CD64^+$, $CD11b^+$, $SigF^-$) from resident AMs ($Dump^-$, $CD45^+$, $CD64^+$, $SigF^+$, $CD11b^-$). Recruited and resident AMs were then interrogated for Arg-1 and IL-10 expression. Cell Counting beads (eBiosciences) were used as an internal reference to quantify the absolute numbers of cells in the lung.[25] All data analysis was performed using Kaluza v.1.5 (Beckman Coulter). UltraComp (eBiosciences) beads were always used to determine instrument voltage settings and compensation settings. Mean Fluorescence intensity was used to quantify Arg-1 and IL-10 expression. The following antibodies were used for flow cytometry experiments: CD45 (BD Biosciences Cat# 550539, RRID:AB_2174426), CD64 (BD Biosciences Cat# 558455, RRID:AB_647241), CD11b (BD Biosciences Cat# 612801, RRID:AB_2870128), Siglec F (SigF) (BD Biosciences Cat# 567600, RRID:AB_2916663), IL-10 (BD Biosciences Cat# 554465, RRID:AB_395410) (all BD Biosciences, Franklin Lakes, NJ, USA), and Arg-1 (Novus Cat# NBP2–03618, RRID:AB_3068632) from Novus Biologicals (Centennial, CO, USA); Labeling kit Alexa-fluor 488 for Arg-1 was from Expedeon/Abcam (Cambridge, UK). Cells were permeabilized for 30 min and incubated with antibody (1:100) for 1 h.

2.16 | Cell culture and treatment

A549 cells (American Type Culture Collection (ATTC), Manassas/VA, USA (ATCC Cat# CRM-CCL-185, RRID:CVCL_0023)) and primary alveolar epithelial type 2 cells (AT II cells) were cultured as described previously[18,26] in Dulbecco's modified Eagle medium (DMEM) with 4.5 g/L glucose and stable L-glutamine, 10% fetal bovine serum (FBS), and 1% penicillin/streptomycin mix (all from Corning Cellgro, Manassas/VA, USA). Primary human airway macrophages were cultured in DMEM with 4.5 g/L glucose and stable L-glutamine, 10% fetal bovine serum (FBS), 1% penicillin/streptomycin mix, and 5 mL Amphotericin B (250 μg/mL). Cells were incubated in a humidified atmosphere of 5% CO_2/95% air at 37°C.

2.17 | Lentiviral generation of cell lines with knockdown of LDHA

A549 cells (RRID:CVCL_0023) with stable decreased expression of LDHA were generated by lentiviral-mediated shRNA expression as described previously.[2] To summarize: pLKO.1 lentiviral vector (Sigma Aldrich RRID:Addgene_8453) targeting LDHA had the shRNA sequence of GCCTGTGCCATCAGTATCTTA (TRCN0000164922). Non-targeting control shRNA (SHC001: Sigma, St Louis/MO, USA) was used as a control. Lentiviral suspensions carrying the plasmid were produced at the Functional Genomics Core Facility of the University of Colorado Boulder. The suspension was used for infection of A549 cells and cells were selected with puromycin (1 μg/mL) for at least two passages before being utilized for downstream experiments.

2.18 | Western blot

Western immunoblotting was used to measure LDHA protein content to confirm stable genetic suppression of LDHA in A549 cells ($A549^{LDHA-/-}$). For Western immunoblotting, cells were washed twice with ice-cold PBS and lysed with 1× cell lysis buffer (Cell Signaling) including protease inhibitor PMSF (effective concentration 100 μg/mL). Protein concentrations were determined using Quickstart Bradford dye reagent (Biorad, Hercules/CA, USA), and equal protein amounts were denatured in sample buffer, separated by SDS-electrophoresis, transferred to a nitrocellulose membrane, blocked in 5% skim milk [w/v] in TBS including 1% Tween-20 [v/v], washed three times with TBST, and then probed with the respective primary antibodies at 4°C overnight. After incubation with primary antibodies, membranes were again washed with TBST 3 for 10 min and then incubated secondary LDHA anti-rabbit (Cell Signaling cat. #7074) or b-actin anti-mouse (cell Signaling cat. #7076) for 1 h. Proteins were detected by ECL (Thermo Fisher Scientific). Actin was used as a loading control. Densitometry was performed with Image J (NIH). Primary antibodies were obtained from: LDHA (Abcam Cat# ab47010, RRID:AB_1952042) and b-actin (Sigma-Aldrich Cat# A5441, RRID:AB_476744).

2.19 | Transcriptional analysis (qPCR)

Total RNA was isolated with Qiagen RNeasy Mini Kit by following the manufacturer's protocol. RNA quantity and purity were measured with Nanodrop 2000 (Gene Company Limited, Hong Kong, China). cDNA was generated using iScript cDNA Synthesis Kit (Bio-Rad, Hercules/CA, USA). RNA transcript levels were determined by real-time RT-PCR (iCycler, Bio-Rad Laboratories Inc.). Primers were obtained from QuantiTect (Qiagen). Mouse: Actinb (QT01136772), IL-6 (QT00098875), CXCL-1(QT00115647), IL-1β (QT01048355), and IL-10 (QT00106169). Human: Actinb (QT01680476), IL-6(QT00083720), and IL-8 (QT00000322).

2.20 | Data analysis

All statistical analyses were carried out using GraphPad Prism 8.1.2 (GraphPad Software, San Diego/CA, USA). All data are expressed as means ± SD, and $p < .05$ was considered statistically significant. For comparison between two groups, two-sample unpaired *t*-tests were used. In cases of comparison between more than two groups, two-way ANOVA and Tukey's multiple comparisons test were applied.

3 | RESULTS

3.1 | Alveolar epithelial cells dampen the release of pro-inflammatory cytokines in macrophages in vitro

We recently showed that the glycolytic shift of ATII cells in response to injurious stimuli protects against experimental ALI.[3] We hypothesized that the metabolic activity of the alveolar epithelium impacts the alveolar macrophage function. To study the interactions between ATII cells and macrophages, we utilized a non-contact co-culture system. For our initial experiments, we utilized bone marrow-derived macrophages (BMDMs) as they are easily obtainable and could be isolated from the same animal as the alveolar type II cells (Figure 1A). Macrophages that were co-cultured with ATII cells displayed a blunted inflammatory response in response to LPS stimulation, as evidenced by decreased transcription of IL-6 and CXCL-1 (Figure 1B,C). We found that ATII-conditioned medium after LPS stimulation that was dialyzed to exclude molecules >3KDa (such as cytokines) decreased fivefold the inflammatory response to LPS stimulation in BMDMs (Figure S1), suggesting that a small molecule such as a metabolic intermediate mediates the quenching of cytokines; these data are in line with studies in tumor-associated macrophages.[10] Incubation with the glycolysis inhibitor dichloroacetic acid prevented the ATII-mediated attenuation of IL-6 and CXCL-1 transcription (Figure 1D,E). Taken together these studies suggest that ATII cells attenuate the inflammatory reaction in macrophages in response to LPS stimulation mediated by the glycolytic pathway.

3.2 | Intra-tracheal lactate shifts alveolar macrophages toward a pro-resolving anti-inflammatory phenotype

We next set out to test whether intratracheal (i.t) administration of exogenous lactate would affect the phenotype of alveolar macrophages in an in vivo model of acute lung injury. To increase the stringency of these experiments, we utilized two murine models of ALI, − i.t hydrochloric acid (HCl) instillation and i.t. instillation of lipopolysaccharide (LPS). Injury develops over days in both models, enabling us to study the effect of i.t. lactate after the onset of the injury.[14,27] After the induction of ALI (6 h), mice received 25 mM of lactate (Figure 2A) while the control group received an equal volume of pH-matched PBS to control for the potential effect of lactic acid reduction in pH (Figure 2A). To study the effects of lactate on different macrophage populations, we isolated alveolar macrophages ($CD64^+$) and then sorted them into recruited ($CD64^+$, $CD11b^+$) and resident macrophages ($CD64^+$, Siglec F^+) (Figure 2B). We found that lactate induced Arg-1 and IL-10 (Figures 2C–F and S2A–C) expression in resident alveolar macrophages. Interestingly, i.t. lactate did not alter the number of resident or recruited airway macrophages in the lung (Figure 2D–F). Furthermore, i.t. lactate given to naïve, non-injured mice did not affect baseline Arg-1 expression (Supplementary Data 3). Our findings suggest that locally administered intra-alveolar lactate can shift the resident alveolar macrophage toward an anti-inflammatory IL-10 and Arg-1 expressing state.

3.3 | Intratracheal lactate given after injurious stimuli attenuates acute lung injury in vivo

We next pursued studies to test whether i.t. lactate would improve ALI overall in murine acid aspiration and LPS models. As described in Figure 2A, ALI was induced and mice

in the treatment group received i.t. lactate 6 h after induction of ALI. The severity of ALI was assessed at 24 h. First, both models of ALI had increased lactate levels in the bronchoalveolar lavage fluid (BALF), which is in line with our previously published results that in response to injury, ATII cells are upregulating their glycolytic activity[3] and thus releasing lactate the end product of glycolysis. Lactate in the BALF was furthermore increased in the treatment group (Figure 3A,H). Histologic analysis revealed that mice that did not receive i.t. lactate had worse lung injury, as evidenced by higher ALI scores compared to controls in both injury models (Figure 3B,C,I,J). This was underscored by the decreased levels of pro-inflammatory cytokine (IL-1β, IL-6, and CXCL-1) mRNA expression in response to i.t. lactate (Figure 3D–F,K–M) in whole lung tissue. Additionally, LPS and acid-induced expression of IL-10 in whole lung tissue was further increased by i.t. lactate (Figure 3G,N). Taken together our findings indicated that i.t.-administrated lactate attenuated ALI severity in two distinct models of ALI by shifting cytokine expression from pro-inflammatory to a more anti-inflammatory state.

3.4 | Alveolar epithelial HIF1A is necessary for the anti-inflammatory differentiation of macrophages in acute lung injury

The transcription factor HIF1A is a critical regulator of glycolysis and hence lactate production in ATII cells.[3] Mice with ATII-specific genetic suppression of Hif1a (*Hif1a*$^{loxp/loxp}$ SPC-Cre-ER+) have a more severe phenotype in several models of acute lung injury.[3,4] Therefore, we investigated whether, in *Hif1a*$^{loxp/loxp}$ SPC-Cre-ER+ mice, the decreased lactate production by ATII cells leads to impaired lactate-mediated paracrine actions between ATII cells and alveolar macrophages. We hypothesized that alveolar macrophages in *Hif1a*$^{loxp/loxp}$ SPC-Cre-ER+ mice would display increased production of pro-inflammatory cytokines and decreased production of anti-inflammatory markers such as IL-10 and Arg-1. Furthermore, we tested whether i.t. lactate could be protective against lung injury in *Hif1a*$^{loxp/loxp}$ SPC-Cre-ER+ mice by reconstituting intra-alveolar lactate levels. In both acid and LPS-induced ALI, we found that *Hif1a*$^{loxp/loxp}$ SPC-Cre-ER+ mice have decreased levels of BALF lactate in response to ALI (Figure 4A,H) compared to SPC-Cre-ER+ control mice. I.t. lactate substitution not only reconstituted BALF lactate in *Hif1a*$^{loxp/loxp}$ SPC-Cre-ER+ mice to levels comparable to SPC-Cre-ER+ controls but improved the severity of ALI as evidenced by a significant decrease in histologic injury severity scores (Figure 4B,C,I,J). Concomitantly, i.t. lactate decreased expression of pro-inflammatory cytokines in *Hif1a*$^{loxp/loxp}$ SPC-Cre-ER+ mice compared to untreated controls (Figure 4D–F,K–M) and increased IL-10 expression (Figure 4G,N) in whole lung homogenate. As i.t. lactate attenuated ALI severity in *Hif1a*$^{loxp/loxp}$ SPC-Cre-ER+ mice in both acid and LPS-induced ALI, we then isolated alveolar macrophages from BALF from *Hif1a*$^{loxp/loxp}$ SPC-Cre-ER+ mice in response to ALI. The ALI-derived *Hif1a*$^{loxp/loxp}$ SPC-Cre-ER+ alveolar macrophages display a more pro-inflammatory phenotype compared to SPC-Cre-ER+ controls (Figure 5A–C,F–I), as evidenced by increased expression of IL-1β, IL-6, and CXCL-1 and decreased IL-10 and Arg-1 expression (Figure 5E,J). Moreover, i.t. lactate significantly suppressed the production of pro-inflammatory cytokines in *Hif1a*$^{loxp/loxp}$ SPC-Cre-ER+ alveolar macrophages, with increased IL-10 and Arg-1 expression to levels similar to the expression of alveolar macrophages from SPC-Cre-ER+ controls (Figure 5D,E,I,J). Taken together, these studies demonstrate that lactate production in ATII cells

under the transcriptional control of HIF1A is both critical and a sufficient suppressor of the inflammatory phenotype of alveolar macrophage in ALI.

3.5 | Pharmacologic inhibition of lactate dehydrogenase A is associated with increased alveolar inflammation

To further explore how lactate affects lung inflammation and hence severity in ALI models, we treated wild-type mice with the pharmacologic lactate dehydrogenase (LDH) A inhibitor FX-11,[28,29] as LDHA catalyzes the conversion from pyruvate to lactate. Based on previous studies,[29,30] mice received 42 μg of FX-11 intra-peritoneally 24 h before acid aspiration to induce ALI. Mice treated with FX-11 displayed exacerbation of ALI including increased protein levels in BALF (Figure 6A), and increased mRNA expression of pro-inflammatory cytokines IL-6 and CXCL-1 in their lungs (Figure 6B,C), leading to exacerbated lung injury based on histologic ALI scores (Figure 6D,E). Taken together, these pharmacologic studies support that inhibition of lactate production with FX-11 leads to worsening lung injury.

3.6 | Epithelial lactate is necessary for macrophage shift in human primary macrophages

As human pulmonary macrophages can have divergent responses to stimuli from murine macrophages,[31,32] we established a human ex vivo approach utilizing primary human alveolar macrophages (AMs) to validate our murine experimental findings. The AM donors included male and female non-smokers and non-diabetics. To exclude donor lungs that had sustained a significant injury, we only utilized lungs with <1% neutrophils in BALF, P/F ratio > 300, clear CXR, and less than 5 days on the ventilator (Figure S4A for sample characteristics). We adjusted the pH of our PBS control to the lactate acid pH utilized in all experiments. To further provide proof of concept of the role of epithelial-produced lactate in a human ex vivo system (Figure 7A), we generated an alveolar epithelial cell line with a stable LDHA knockdown ($A549^{LDHA-/-}$) (Figure S4B). $A549^{LDHA-/-}$ cells had decreased lactate concentration in cell culture supernatant in response to LPS stimulation (Figure 7B). We found the primary human AMs that were co-cultured with $A549^{LDHA-/-}$ cells displayed increased levels of pro-inflammatory cytokines IL-6 and IL-8 when stimulated with LPS, similar to macrophages that were cultured without epithelial cells. In contrast, primary human AM co-cultured with A549 control cells (A549 scr) displayed not only blunted inflammatory cytokine response to LPS stimulation but also increased transcription of the IL-10 and Arg-1 mRNA (Figure 7C–F), which are markers associated with an anti-inflammatory proresolving state.[10,33] In summary, these findings indicate that lactate produced by the alveolar epithelium under injurious conditions such as treatment with LPS can shape the phenotype of primary human AMs toward a more anti-inflammatory state.

4 | DISCUSSION

While lactate was thought to represent an intermediate metabolite resulting from glycolysis, lactate also has an expanded role as an anaplerotic substrate (a major source of energy and gluconeogenic precursors) and also as a signaling molecule.[34] While peripheral elevated blood lactate levels in the clinical setting are often seen as a sign of poor tissue perfusion, localized elevated lactate levels can be beneficial.[33,35,36] Inflammation can be associated with high concentrations of lactate, which can be transported from intracellular sources to

the immediate and distant extracellular space. Lactate can then be taken up by effector cells and used as a metabolic substrate. There is growing evidence that changes in metabolic flux and signaling through metabolic intermediates play critical roles in AM phenotypes.[37,38] As our murine ALI models directly target the intra-alveolar space and hence the alveolar epithelium, we focused on the effect of lactate produced by the alveolar epithelium on AMs, as they reside in close proximity to the epithelium. We set out to delineate the role of lactate-mediated metabolic cross-talk between ATII and AMs in acute lung injury, dissecting how lactate produced by ATII cells can counter-regulate excessive inflammation by shifting the alveolar macrophage phenotype toward anti-inflammatory and potentially pro-resolving activity. Our data indicate that in ATII cells, HIF1A-mediated augmented production of lactate can act as an innate protective mechanism. Locally intratracheally instilled lactate decreases pulmonary inflammation and thus attenuates ALI in two different murine models of lung injury. Additionally, with a translational approach utilizing primary human alveolar macrophages, we show that ATII-produced lactate is necessary to counteract the pro-inflammatory activation of AMs.

Macrophages can reversibly switch their inflammatory state depending on their environment; pro-inflammatory macrophages are characterized by efficient antigen presentation, high bactericidal activity, and the production of pro-inflammatory cytokines and reactive oxygen and nitrogen species. In contrast, pro-resolving macrophages execute immune-regulatory functions by releasing anti-inflammatory cytokines and decreasing the production of pro-inflammatory cytokines. As AMs reside in the alveolar space near ATII cells,[5] the phenotype of the AM is affected by the local microenvironmental (metabolites, cytokines, and surrounding cells) that shape their inflammatory or anti-inflammatory properties, which are fluent and amenable to manipulation.[6,9] We showed that in the intra-alveolar niche, lactate produced by ATII can shift the AM phenotype toward an anti-inflammatory phenotype. While there is extensive literature characterizing different pulmonary macrophage phenotype subsets by bulk RNA or single-cell sequencing,[11,39] we demonstrate the shift of the AMs to a more anti-inflammatory phenotype in response to lactate by cytokine production, which together with your histologic characterization of ALI represents a more physiologic phenotypic switch.

Maintenance of tissue homeostasis is a major function of macrophages.[40] Cross-talk between tissue macrophages and their neighboring cells has been described in the context of cancer, where lactate produced by tumor cells can shift polarization of surrounding tumor-associated macrophages to an anti-inflammatory, pro-resolving phenotype and thus allow tumor maintenance and growth.[41,42] In contrast to cancer, lactate-mediated crosstalk between the endothelium and tissue macrophages was found to be beneficial by improving muscle regeneration in a murine model of hindlimb ischemia as lactate enhanced the ability of macrophages to adopt a proangiogenic and pro-regenerative M2-like phenotype.[43] Interestingly, this study demonstrated that 6-phosphofructo-2-kinase/fructose-2,6-bisphosphatase (PFKFB) 3 is the driver of the macrophage phenotype, which is in line with the protective role of ATII cell PFKFB3 in ALI.[3] These findings are consistent with our observations that lactate produced by the alveolar epithelium can shift the alveolar macrophages from a pro-inflammatory toward an anti-inflammatory, pro-resolving phenotype. Moreover, our findings indicate that exogenous, locally applied i.t. lactate can

enhance this innate protective pathway, as i.t. lactate was able to attenuate ALI in two different models of ALI.

While AMs lavaged from inflamed lungs were once considered a homogeneous cell type, two ontogenetically distinct populations of alveolar macrophages co-exist in the inflamed lung: resident AMs, which are fetal monocyte derived and maintained via self-renewal, and recruited AMs, which originate postnatally from circulating monocytes.[11,38] Less well described in the context of ALI are interstitial macrophages.[44,45] However, we speculate that the effect of lactate is dependent on the specific lung compartment. This could explain why in our direct ALI models (i.t. LPS or acid aspiration) which target the alveolar epithelium and Ams, the effect of lactate is protective, whereas in a model of indirect lung ALI (LPS endotoxemia), inhibition of glycolysis attenuated lung injury.[46] Interestingly, our findings showed that i.t. lactate shifted the phenotype of the resident AMs but not the recruited AMs. One possible explanation for this could be the early time point of our experiments, with a relatively low number of recruited AMs having reached the intra-alveolar space (Figure S2C).

The transcription factor HIF1A is a major driver of glycolysis.[47,48] Furthermore, alveolar epithelial-specific deletion of HIF1a has been associated with worse outcomes in ALI in several murine models of ALI and decreased lactate production in ATII cells.[2–4] This is in line with our findings that *Hif1a*$^{loxp/loxp}$ SPC-Cre-ER+ mice have decreased lactate levels in BALF. Treating the *Hif1a*$^{loxp/loxp}$ SPC-Cre-ER+ mice with i.t. lactate after the onset of ALI resulted in a shift of the AM toward an anti-inflammatory phenotype and decreased inflammation and improved ALI, which was associated with increased levels of alveolar lactate.

Glycolysis is one of the major metabolic pathways that is activated in the setting of inflammation.[49–52] Its end product, pyruvate, in the setting of cellular stressors associated with ALI (such as hypoxia or increased macromolecular biosynthesis), can be diverted away from oxidative phosphorylation. There is ample evidence of the pro-inflammatory effects of lactate: for example, in in vitro models, lactate produced by glycolysis has been shown to increase TNFα secretion[53] and enhance TLR4 signaling and NFKb signaling thus augmenting cytokine production.[54,55] However, there is growing evidence that lactate can also have anti-inflammatory effects. For example, efferocytosis-induced production of lactate has been shown to induce the expression of anti-inflammatory, pro-resolving genes such as Tgfb and IL-10,[56] delay the inflammatory response in monocytes,[57] and inhibit pro-inflammatory cytokine production via GPR18 in vitro and a murine pancreatitis model. Interestingly, a short-term infusion of lactate in humans in vivo increased ex vivo glucose consumption of PBMCs, but only mildly affected cytokine production. However, the same study showed that long-term treatment with lactate ex vivo, reflecting pathophysiological conditions in local microenvironments such as tumor or inflammation shifted cytokine production towards an anti-inflammatory state.[58] Lastly, as murine and human pulmonary macrophages can have diverging responses to stimuli,[31,32] we also established a human ex vivo approach utilizing primary human alveolar macrophages to validate our findings in murine ALI. We could recapitulate our in vitro and in vivo observations in primary human cells thus underscoring the translational potential of our findings, although our

findings are limited by a small sample size and will need to be validated in a bigger cohort beyond the scope of this work. Furthermore, our co-culture system human A549, and primary human AMs enabled us to selectively inhibit LDHA and hence suppress lactate production in the alveolar epithelial cells. Primary human AM co-cultured with alveolar epithelial cells with diminished capacity to produce lactate ($A549^{LDHA-/-}$) did not display the anti-inflammatory, pro-resolving phenotype that was observed in native A549- primary human AM co-culture, hence underscoring that lactate produced by alveolar epithelial cells is critical for the AM phenotype. Although the exact mechanisms by which lactate can quench inflammation are still unknown, new and exciting studies have identified a role for lactate in histone modification as a driver for macrophage differentiation.[59,60]

Taken together, our studies identify a protective role of lactate-mediated cross-talk between ATII cells and alveolar macrophages in acute lung injury. The current studies contribute to the understanding of how manipulation of inflammation, one of the key pathophysiologic components of ALI by shaping the phenotype of alveolar macrophages, could be a new strategy in the treatment of ALI/ARDS.

Supplementary Material

Refer to Web version on PubMed Central for supplementary material.

ACKNOWLEDGMENTS

We would like to thank Dr. Patrick Hume and Dr. William B. Janssen from the National Jewish Hospital for their help in obtaining the human BALF samples.

FUNDING INFORMATION

This work was supported by National Institute of Health Grant K12HD068372, K08HL130586, Society of Critical Care Medicine Weil Discovery grant, and Parker B. Francis Fellowship to CUV. R35HL139726 to ENS and PO1HL152961 to KS and RT (Project 3).

HHS | NIH | Eunice Kennedy Shriver National Institute of Child Health and Human Development (NICHD), Grant/Award Number: K12HD068372; HHS | NIH | National Heart, Lung, and Blood Institute (NHLBI), Grant/Award Number: R35HL139726 and PO1HL152961; HHS | NIH | NHLBI | NHLBI Division of Intramural Research (DIR), Grant/Award Number: K08HL130586; Parker B Francis; Society of Critical Care Medicine (SCCM)

DATA AVAILABILITY STATEMENT

Data sharing is not applicable to this article as no datasets were generated or analyzed during the current study.

Abbreviations:

ALI	Acute lung injury
AM	Alveolar macrophage
ANOVA	Analysis of variance
ARDS	Acute respiratory distress syndrome
ATII	Alveolar type II cells

BAL	Bronchoalveolar lavage
BALF	Bronchoalveolar Lavage Fluid
BMDM	Bone marrow derived macrophages
DAPI	4’,6-diamidino-2-phenylindole
EDTA	Ethylenediaminetetraacetic acid
HEPES	4–2-hydroxyethyl-1piperazineethansulfonic acid
DCA	Dichloracetic acid
DMEM	Dulbeccco Modified Eagle Medium
FBS	Fetal bovine serum
H&E	Hematoxilin and Eosin
HIF	Hypoxia Inducible Factor
LDH	Lactate dehydrogenase
LPS	Lipopolysacceride
MFI	Mean fluorescence intensity
PBS	Phosphate buffered saline
PFKFB3	Phosphofructokinase-2/fructose-2,6-bisphosphatase 3
VEGF	Vascular endothelial growth factor

REFERENCES

1. Elks PM, van Eeden FJ, Dixon G, et al. Activation of hypoxia-inducible factor-1alpha (Hif-1alpha) delays inflammation resolution by reducing neutrophil apoptosis and reverse migration in a zebrafish inflammation model. Blood 2011;118:712–722. [PubMed: 21555741]
2. Eckle T, Brodsky K, Bonney M, et al. HIF1A reduces acute lung injury by optimizing carbohydrate metabolism in the alveolar epithelium. PLoS Biol 2013;11:e1001665. [PubMed: 24086109]
3. Vohwinkel CU, Burns N, Coit E, et al. HIF1A-dependent induction of alveolar epithelial PFKFB3 dampens acute lung injury. JCI Insight 2022;7:e157855. doi:10.1172/jci.insight.157855 [PubMed: 36326834]
4. Vohwinkel CU, Coit EJ, Burns N, et al. Targeting alveolar-specific succinate dehydrogenase a attenuates pulmonary inflammation during acute lung injury. FASEB J 2021;35:e21468. [PubMed: 33687752]
5. Bain CC, MacDonald AS. The impact of the lung environment on macrophage development, activation and function: diversity in the face of adversity. Mucosal Immunol 2022;15:223–234. [PubMed: 35017701]
6. Martin FP, Jacqueline C, Poschmann J, Roquilly A. Alveolar macrophages: adaptation to their anatomic niche during and after inflammation. Cell 2021;10:2720. doi:10.3390/cells10102720
7. Herold S, Mayer K, Lohmeyer J. Acute lung injury: how macrophages orchestrate resolution of inflammation and tissue repair. Front Immunol 2011;2:65. [PubMed: 22566854]

8. Huang X, Xiu H, Zhang S, Zhang G. The role of macrophages in the pathogenesis of ALI/ARDS. Mediators Inflamm 2018;2018:1264913. [PubMed: 29950923]
9. Puttur F, Gregory LG, Lloyd CM. Airway macrophages as the guardians of tissue repair in the lung. Immunol Cell Biol 2019;97:246–257. [PubMed: 30768869]
10. Colegio OR, Chu NQ, Szabo AL, et al. Functional polarization of tumour-associated macrophages by tumour-derived lactic acid. Nature 2014;513:559–563. [PubMed: 25043024]
11. Mould KJ, Moore CM, McManus SA, et al. Airspace macrophages and monocytes exist in transcriptionally distinct subsets in healthy adults. Am J Respir Crit Care Med 2021;203:946–956. [PubMed: 33079572]
12. Rock JR, Barkauskas CE, Cronce MJ, et al. Multiple stromal populations contribute to pulmonary fibrosis without evidence for epithelial to mesenchymal transition. Proc Natl Acad Sci U S A 2011;108:E1475–E1483. [PubMed: 22123957]
13. Madisen L, Zwingman TA, Sunkin SM, et al. A robust and high-throughput Cre reporting and characterization system for the whole mouse brain. Nat Neurosci 2010;13:133–140. [PubMed: 20023653]
14. Hoegl S, Burns N, Angulo M, et al. Capturing the multifactorial nature of ARDS – "two-hit" approach to model murine acute lung injury. Physiol Rep 2018;6:e13648. [PubMed: 29595879]
15. Patel BV, Wilson MR, Takata M. Resolution of acute lung injury and inflammation: a translational mouse model. Eur Respir J 2012;39:1162–1170. [PubMed: 22005920]
16. Beck JM, Preston AM, Wilcoxen SE, Morris SB, Sturrock A, Paine R 3rd. Critical roles of inflammation and apoptosis in improved survival in a model of hyperoxia-induced acute lung injury in Pneumocystis murina-infected mice. Infect Immun 2009;77:1053–1060. [PubMed: 19124601]
17. Mercer PF, Johns RH, Scotton CJ, et al. Pulmonary epithelium is a prominent source of proteinase-activated receptor-1-inducible CCL2 in pulmonary fibrosis. Am J Respir Crit Care Med 2009;179:414–425. [PubMed: 19060230]
18. Hoffman O, Burns N, Vadasz I, Eltzschig HK, Edwards MG, Vohwinkel CU. Detrimental ELAVL-1/HuR-dependent GSK3beta mRNA stabilization impairs resolution in acute respiratory distress syndrome. PloS One 2017;12:e0172116. [PubMed: 28196122]
19. Good RJ, Hernandez-Lagunas L, Allawzi A, et al. MicroRNA dysregulation in lung injury: the role of the miR-26a/EphA2 axis in regulation of endothelial permeability. Am J Physiol Lung Cell Mol Physiol 2018;315:L584–L594. [PubMed: 30024304]
20. Herold S, von Wulffen W, Steinmueller M, et al. Alveolar epithelial cells direct monocyte transepithelial migration upon influenza virus infection: impact of chemokines and adhesion molecules. J Immunol 2006;177:1817–1824. [PubMed: 16849492]
21. Koppe U, Hogner K, Doehn JM, et al. Streptococcus pneumoniae stimulates a STING- and IFN regulatory factor 3-dependent type I IFN production in macrophages, which regulates RANTES production in macrophages, cocultured alveolar epithelial cells, and mouse lungs. J Immunol 2012;188:811–817. [PubMed: 22156592]
22. Ehrentraut H, Clambey ET, McNamee EN, et al. $CD73^{+}$ regulatory T cells contribute to adenosine-mediated resolution of acute lung injury. FASEB J 2013;27:2207–2219. [PubMed: 23413361]
23. Maeda M, Ozaki T, Yasuoka S, Ogura T. Role of alveolar macrophages and neutrophils in the defense system against infection of Pseudomonas aeruginosa in the respiratory tract and the effect of derivative of muramyl dipeptide. Nihon Kyobu Shikkan Gakkai Zasshi 1990;28:135–142. [PubMed: 2355674]
24. Allawzi A, McDermott I, Delaney C, et al. Redistribution of EC-SOD resolves bleomycin-induced inflammation via increased apoptosis of recruited alveolar macrophages. FASEB J 2019;33:13465–13475. [PubMed: 31560857]
25. Pugliese SC, Kumar S, Janssen WJ, et al. A time- and compartment-specific activation of lung macrophages in hypoxic pulmonary hypertension. J Immunol 2017;198:4802–4812. [PubMed: 28500078]
26. Vohwinkel CU, Buchackert Y, Al-Tamari HM, et al. Restoration of Megalin-mediated clearance of alveolar protein as a novel therapeutic approach for acute lung injury. Am J Respir Cell Mol Biol 2017;57:589–602. [PubMed: 28678521]

27. Kulkarni HS, Lee JS, Bastarache JA, et al. Update on the features and measurements of experimental acute lung injury in animals: an official American Thoracic Society workshop report. Am J Respir Cell Mol Biol 2022;66:e1–e14. [PubMed: 35103557]
28. Deck LM, Royer RE, Chamblee BB, et al. Selective inhibitors of human lactate dehydrogenases and lactate dehydrogenase from the malarial parasite Plasmodium falciparum. J Med Chem 1998;41:3879–3887. [PubMed: 9748363]
29. Le A, Cooper CR, Gouw AM, et al. Inhibition of lactate dehydrogenase a induces oxidative stress and inhibits tumor progression. Proc Natl Acad Sci U S A 2010;107:2037–2042. [PubMed: 20133848]
30. Dutta P, Le A, Vander Jagt DL, et al. Evaluation of LDH-A and glutaminase inhibition in vivo by hyperpolarized 13C-pyruvate magnetic resonance spectroscopy of tumors. Cancer Res 2013;73:4190–4195. [PubMed: 23722553]
31. Ogger PP, Byrne AJ. Macrophage metabolic reprogramming during chronic lung disease. Mucosal Immunol 2021;14:282–295. [PubMed: 33184475]
32. Vijayan V, Pradhan P, Braud L, et al. Human and murine macrophages exhibit differential metabolic responses to lipopolysaccharide—a divergent role for glycolysis. Redox Biol 2019;22:101147. [PubMed: 30825774]
33. Ivashkiv LB. The hypoxia-lactate axis tempers inflammation. Nat Rev Immunol 2020;20:85–86. [PubMed: 31819164]
34. Brooks GA. The science and translation of lactate shuttle theory. Cell Metab 2018;27:757–785. [PubMed: 29617642]
35. Chen AN, Luo Y, Yang YH, et al. Lactylation, a novel metabolic reprogramming code: current status and prospects. Front Immunol 2021;12:688910. [PubMed: 34177945]
36. De Bock K, Georgiadou M, Schoors S, et al. Role of PFKFB3-driven glycolysis in vessel sprouting. Cell 2013;154:651–663. [PubMed: 23911327]
37. Errea A, Cayet D, Marchetti P, et al. Lactate inhibits the pro-inflammatory response and metabolic reprogramming in murine macrophages in a GPR81-independent manner. PloS One 2016;11:e0163694. [PubMed: 27846210]
38. Mould KJ, Barthel L, Mohning MP, et al. Cell origin dictates programming of resident versus recruited macrophages during acute lung injury. Am J Respir Cell Mol Biol 2017;57:294–306. [PubMed: 28421818]
39. Mould KJ, Jackson ND, Henson PM, Seibold M, Janssen WJ. Single cell RNA sequencing identifies unique inflammatory airspace macrophage subsets. JCI Insight 2019;4:e126556. doi:10.1172/jci.insight.126556 [PubMed: 30721157]
40. Pollard JW. Trophic macrophages in development and disease. Nat Rev Immunol 2009;9:259–270. [PubMed: 19282852]
41. Grivennikov SI, Greten FR, Karin M. Immunity, inflammation, and cancer. Cell 2010;140:883–899. [PubMed: 20303878]
42. Qian BZ, Pollard JW. Macrophage diversity enhances tumor progression and metastasis. Cell 2010;141:39–51. [PubMed: 20371344]
43. Zhang J, Muri J, Fitzgerald G, et al. Endothelial lactate controls muscle regeneration from ischemia by inducing M2-like macrophage polarization. Cell Metab 2020;31:1136–1153 e1137. [PubMed: 32492393]
44. Hou F, Xiao K, Tang L, Xie L. Diversity of macrophages in lung homeostasis and diseases. Front Immunol 2021;12:753940. [PubMed: 34630433]
45. Schyns J, Bureau F, Marichal T. Lung interstitial macrophages: past, present, and future. J Immunol Res 2018;2018:5160794. [PubMed: 29854841]
46. Wang L, Cao Y, Gorshkov B, et al. Ablation of endothelial Pfkfb3 protects mice from acute lung injury in LPS-induced endotoxemia. Pharmacol Res 2019;146:104292. [PubMed: 31167111]
47. Corcoran SE, O'Neill LA. HIF1alpha and metabolic reprogramming in inflammation. J Clin Invest 2016;126:3699–3707. [PubMed: 27571407]
48. Vohwinkel CU, Hoegl S, Eltzschig HK. Hypoxia signaling during acute lung injury. J Appl Physiol (1985) 2015;119:1157–1163. [PubMed: 25977449]

49. Kominsky DJ, Campbell EL, Colgan SP. Metabolic shifts in immunity and inflammation. J Immunol 2010;184:4062–4068. [PubMed: 20368286]
50. O'Neill LA, Kishton RJ, Rathmell J. A guide to immunometabolism for immunologists. Nat Rev Immunol 2016;16:553–565. [PubMed: 27396447]
51. Taylor CT, Colgan SP. Hypoxia and gastrointestinal disease. J Mol Med (Berl) 2007;85:1295–1300. [PubMed: 18026919]
52. Taylor CT, Colgan SP. Regulation of immunity and inflammation by hypoxia in immunological niches. Nat Rev Immunol 2017;17:774–785. [PubMed: 28972206]
53. Dietl K, Renner K, Dettmer K, et al. Lactic acid and acidification inhibit TNF secretion and glycolysis of human monocytes. J Immunol 2010;184:1200–1209. [PubMed: 20026743]
54. Nareika A, He L, Game BA, et al. Sodium lactate increases LPS-stimulated MMP and cytokine expression in U937 histiocytes by enhancing AP-1 and NF-kappaB transcriptional activities. Am J Physiol Endocrinol Metab 2005;289:E534–E542. [PubMed: 15941782]
55. Samuvel DJ, Sundararaj KP, Nareika A, Lopes-Virella MF, Huang Y. Lactate boosts TLR4 signaling and NF-kappaB pathway-mediated gene transcription in macrophages via monocarboxylate transporters and MD-2 up-regulation. J Immunol 2009;182:2476–2484. [PubMed: 19201903]
56. Morioka S, Perry JSA, Raymond MH, et al. Efferocytosis induces a novel SLC program to promote glucose uptake and lactate release. Nature 2018;563:714–718. [PubMed: 30464343]
57. Peter K, Rehli M, Singer K, Renner-Sattler K, Kreutz M. Lactic acid delays the inflammatory response of human monocytes. Biochem Biophys Res Commun 2015;457:412–418. [PubMed: 25582773]
58. Ratter JM, Rooijackers HMM, Hooiveld GJ, et al. In vitro and in vivo effects of lactate on metabolism and cytokine production of human primary PBMCs and monocytes. Front Immunol 2018;9:2564. [PubMed: 30483253]
59. Noe JT, Rendon BE, Geller AE, et al. Lactate supports a metabolic-epigenetic link in macrophage polarization. Sci Adv 2021;7:eabi8602.
60. Zhang D, Tang Z, Huang H, et al. Metabolic regulation of gene expression by histone lactylation. Nature 2019;574:575–580. [PubMed: 31645732]

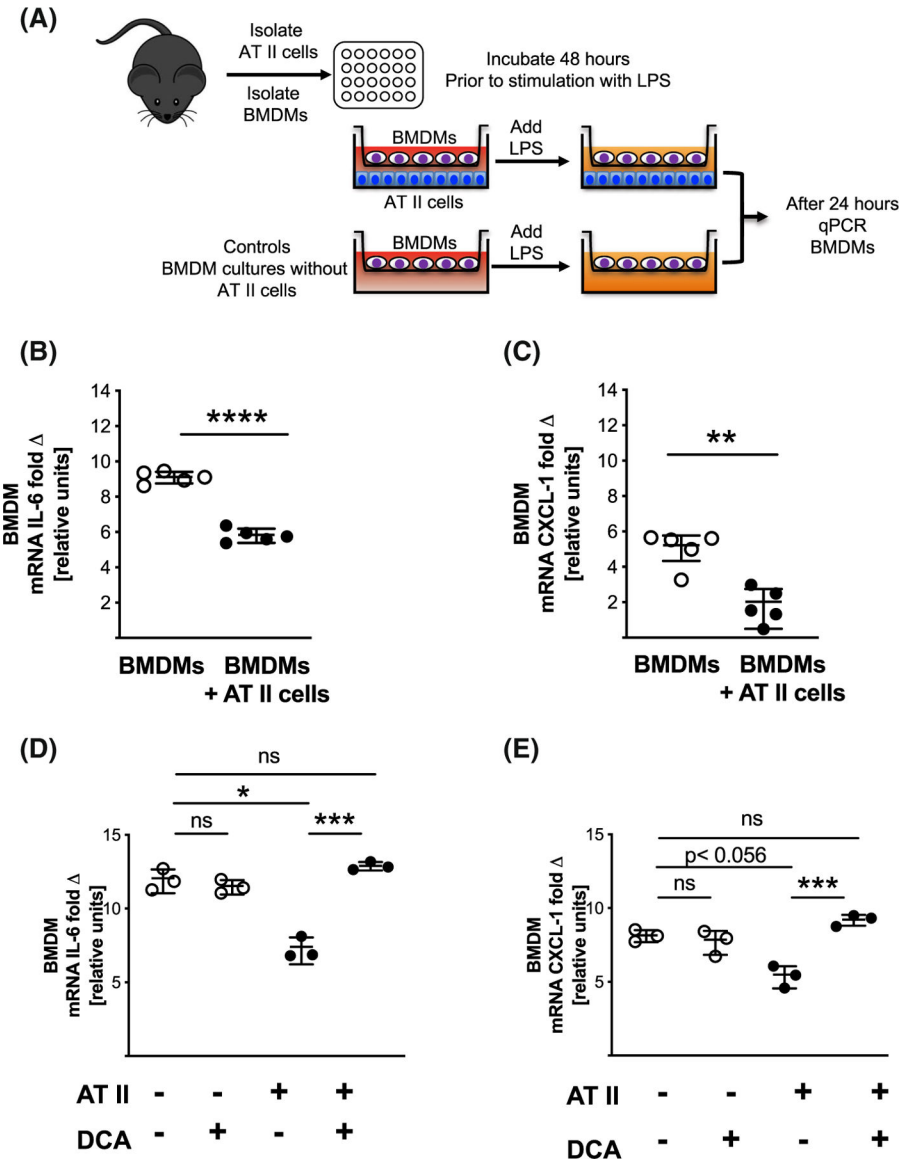

FIGURE 1.

AT II cells suppress cytokine release in macrophages. Schematic of macrophages–AT II co-culture system (A): AT I cells and BMDMs were isolated from the same animal and incubated in a non-contact insert co-culture system for 48 h prior to stimulation with 50 ng/mL LPS. Twenty-four hours after LPS stimulation, BMDMs were harvested. mRNA expression of IL-6 (B) and CXCL1 (C) was determined with qPCR in BMDMs cultured with and without ATIIs (Controls) after 24 h. BMDM cells were cultured either alone or co-cultured with AT II cells with respective controls and incubated with 2.5 mM of glycolysis inhibitor dichloroacetic acid (DCA) and stimulated with LPS. After 24 h, cytokine mRNA expression was determined with qPCR (D, E). $n = -5$, data expressed as mean ± SD, $^{*}p < .05$, $^{**}p < .01$, $^{***}p < .001$, $^{****}p < .0001$. Data were analyzed with two-tailed, unpaired, Student's *t*-test (B, C) or one-way ANOVA with Tukey's correction for multiple comparisons (D, E).

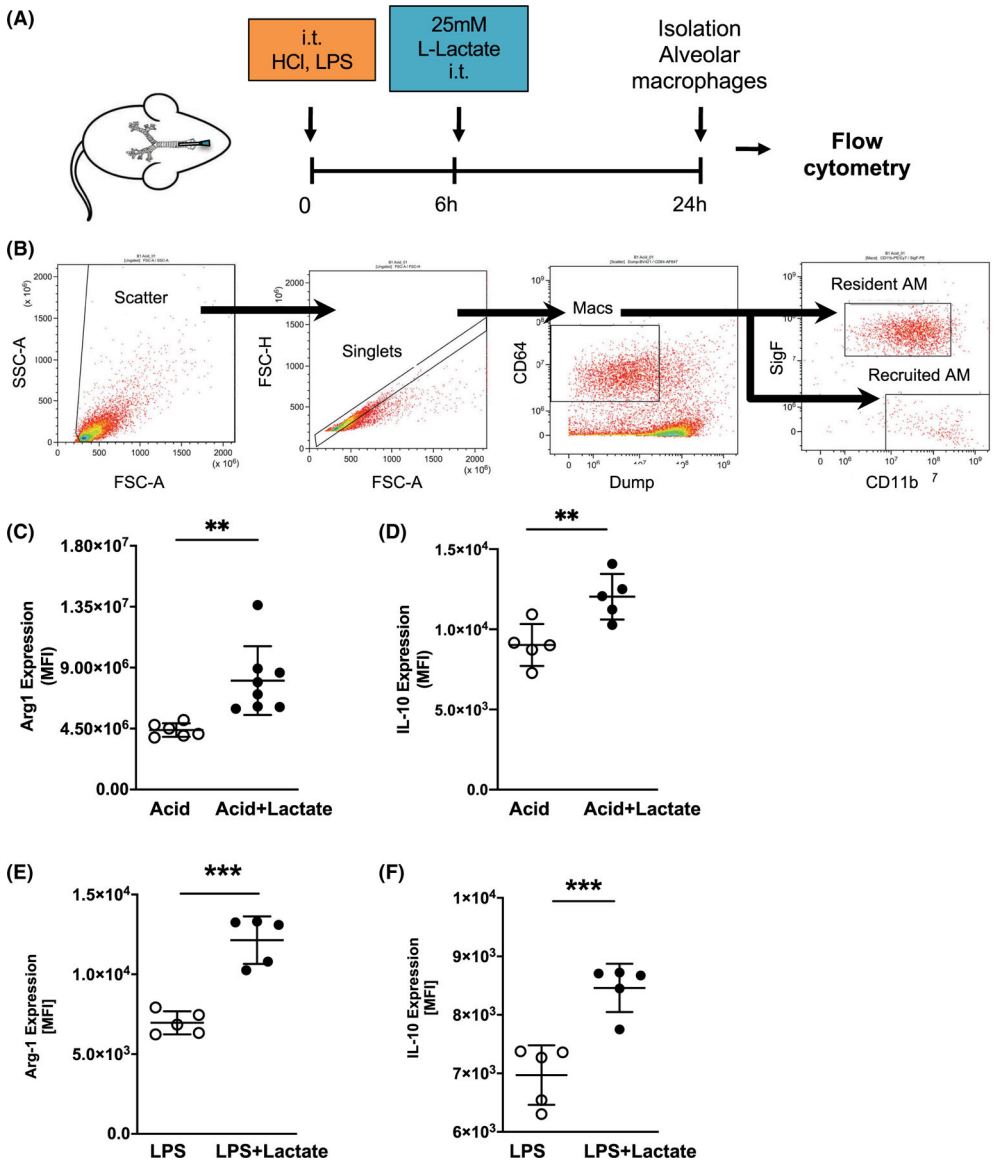

FIGURE 2.

Intratracheal L-lactate shifts resident macrophages pro-resolving phenotype. Schematic of mouse experiments: Acute lung injury was induced by either 0.125 M HCl (Acid) or 5 μ/g intratracheal (i.t.) LPS. Six hours after the induction of lung injury, mice received 50 μL 25 mM L-lactate. The injury control group received 50 μL pH-controlled PBS. Age-, sex-, and weight-matched C57/B6 mice were used. The experiment was terminated after 24 h (A). Flow cytometry sorting strategy. Monocytes, neutrophils, B cells, and T cells were excluded. $CD45^+$ population was then segregated into resident AMs ($Dump^-$, $CD45^+$, $CD64^+$, $SigF^+$, $CD11b^-$) and recruited AMs ($CD45^+$, $CD64^+$, $SigF^-$, $CD11b^+$) (B). Arg-1 expression (C, E), respectively, IL-10 expression (G, F) in resident airway macrophages were determined by flow cytometry and expressed as mean fluorescence intensity (MFI). $n = 5–7$, data expressed as mean ± SD, $^{**}p < .01$, $^{***}p < .001$. Data were analyzed with two-tailed, unpaired, Student's *t*-test.

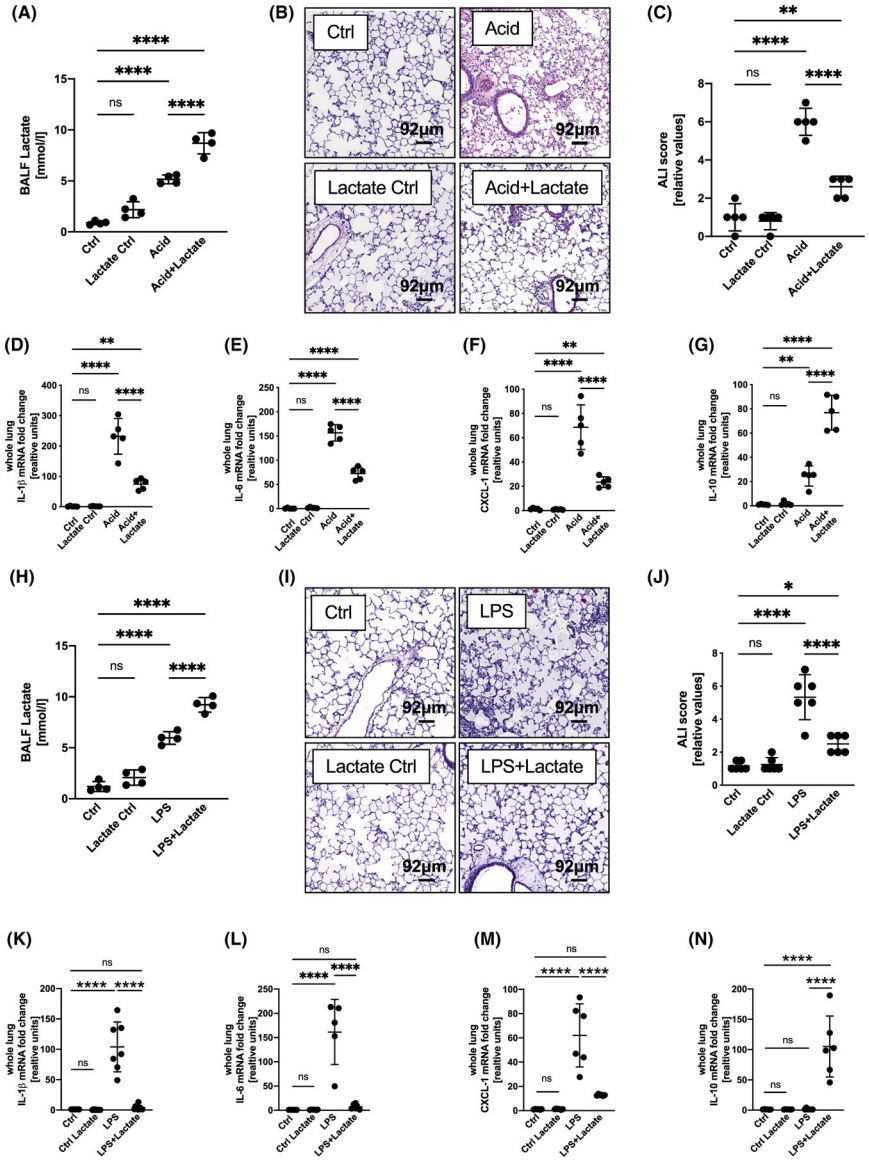

FIGURE 3.

Intratracheal L-lactate attenuates acute lung injury. Acute lung injury was induced in age-, sex-, and weight-matched C57/B6 mice by 5 µ/g intratracheal (i.t.) LPS (A–G) or 0.125 M HCl i.t. (H–N) 6 h after the induction of lung injury mice received 50 µL 25 mM L-lactate (LPS+ lactate). The injury control group received 50 µL pH-controlled PBS. Lactate was measured in bronchoalveolar lavage fluid (BALF) at the end of the experiment (A, H). Representative images of H&E-stained lungs (B, I). A semi-quantitative cumulative lung injury score was performed, which is a combined score of cellular infiltrates, interstitial congestion, hyaline membrane formation, and hemorrhage (C, J). mRNA expression in whole lung tissue was determined by qPCR (D–G and K–N). $n = 4–6$/group. Data are represented as mean ± SD, ns = not significant, $^{**}p < .01$, $^{****}p < .0001$. Data were analyzed with one-way ANOVA with Tukey's correction for multiple comparisons.

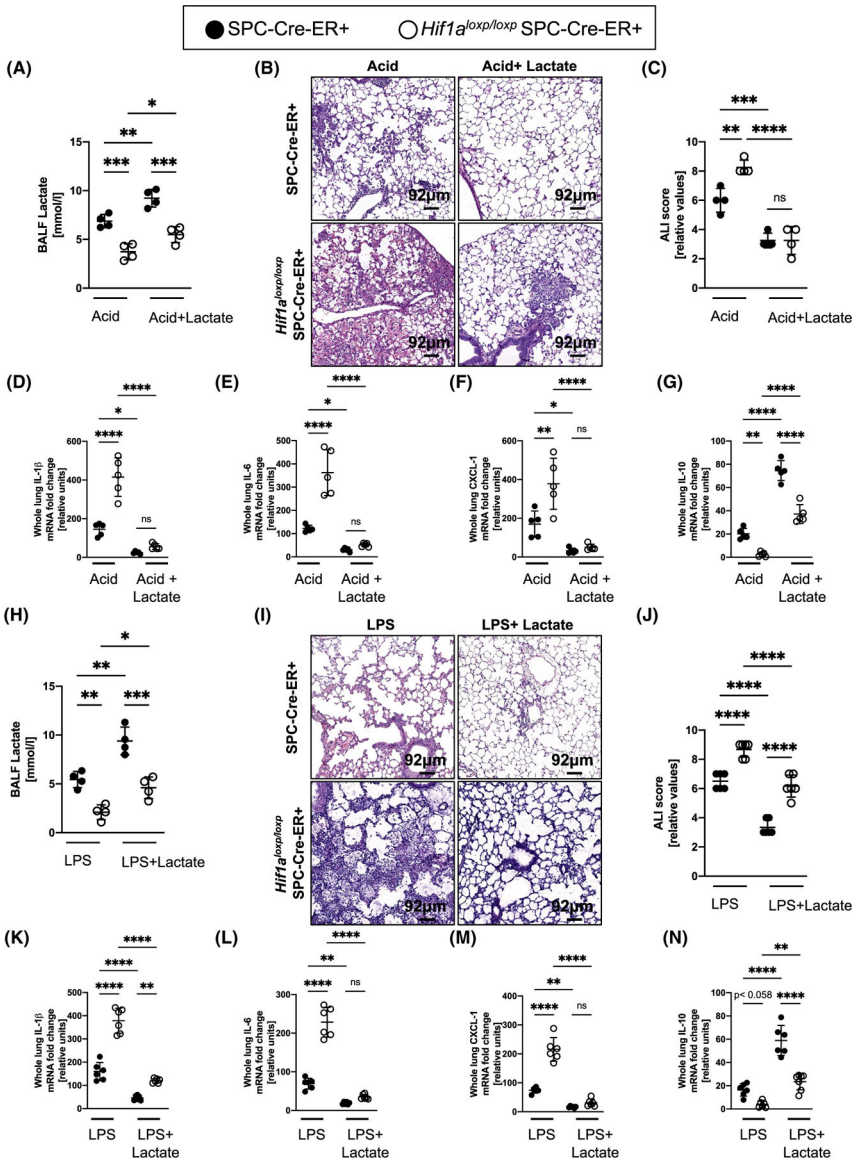

FIGURE 4.

Intra-tracheal L-lactate reconstitutes *Hif1a*$^{loxp/loxp}$ SPC-ER-Cre+ animals. Acute lung injury was induced in age-, sex-, and weight-matched alveolar epithelial cell-specific conditional knockout mice (*Hif1a*$^{loxp/loxp}$ SPC-ER-Cre+ or control animals (SPC-ER-Cre+) by 5 µ/g intratracheal (i.t.) LPS (A–G) or 0.125 M HCl (H–N) i.t. 6 h after the induction of lung injury mice received 50 µL 25 mM L-lactate (LPS+ lactate). The injury control group received 50 µL pH-controlled PBS. Lactate was measured in bronchoalveolar lavage fluid (BALF) at the end of the experiment (A, H). Representative images of H&E-stained lungs (B, I). A semi-quantitative cumulative lung injury score was performed, which is a combined score of cellular infiltrates, interstitial congestion, hyaline membrane formation, and hemorrhage (C, J). mRNA expression in whole lung tissue was determined by qPCR (D–G and K–N). n = 4–6/group. Data are represented as mean ± SD, ns = not significant, *p

< .05, **p < .01, ***p < .001, ****p < .0001. Data were analyzed with one-way ANOVA with Tukey's correction for multiple comparisons.

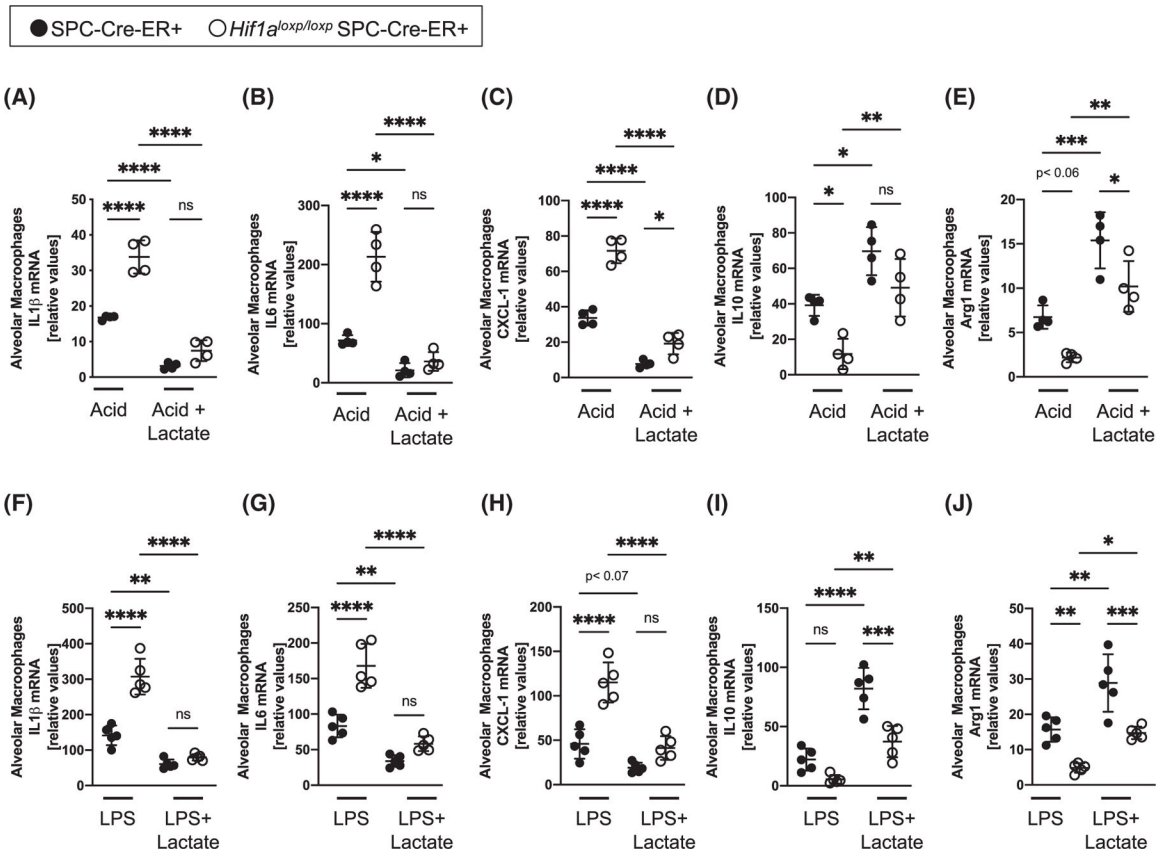

FIGURE 5.

Mice with alveolar type 2 specific suppression of *Hif1a* are unable to shift resident macrophages' pro-resolving phenotype in response to ALI. Acute lung injury was induced by intratracheal LPS (A–E) or HCl (G–J) in *Hif1a*$^{loxp/loxp}$ surfactant Cre+ (*Hif1a*$^{loxp/loxp}$ SPC-ER-Cre+) mice in age-, sex-, and weight-matched controls (SPC-ER-Cre+). Six hours after the induction of lung injury, mice received 50 μL 25 mM L-lactate with control group receiving 50 μL pH-controlled PBS. Twenty-four hours after induction of ALI, the AMs were harvested by bronchoalveolar lavage. mRNA expression in airway macrophages was determined by qPCR. n = 4–5/group. Data are represented as mean ± SD, ns = not significant, *$p < .05$, **$p < .01$, ***$p < .001$, ****$p < .0001$. Data were analyzed with one-way ANOVA with Tukey's correction for multiple comparisons.

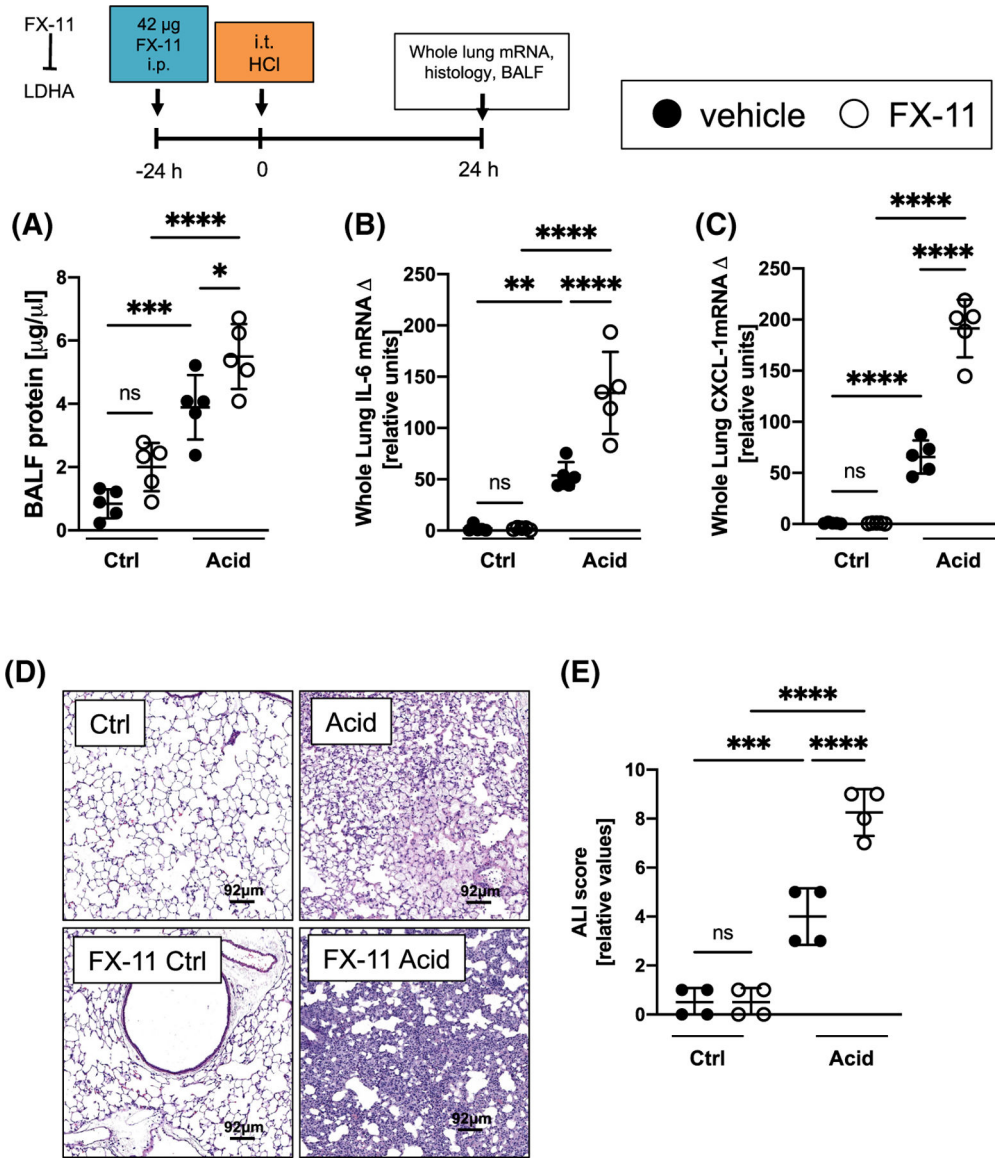

FIGURE 6.

Pharmacological inhibition of LDHA exacerbates acid aspiration-induced acute lung injury. Eight- to 10-week-old C57BL/6 mice received LDHA inhibitor FX-11 i.p 24 h prior to induction of ALI with acid instillation with i.t. HCl. Control groups received vehicle. After 24 h, the lungs were removed. Protein concentration was measured in BALF with Bradford-assay (A). mRNA expression in whole lung tissue was determined by qPCR (B, C). Representative images of H&E-stained lungs (D). A semi-quantitative cumulative lung injury score was performed, which is a combined score of cellular infiltrates, interstitial congestion, hyaline membrane formation, and hemorrhage (E) $n = 4–5$/group. Data are represented as mean ± SD, ns = not significant, *$p < .05$, **$p < .01$, ***$p < .001$, ****$p < .0001$. Data were analyzed with one-way ANOVA with Tukey's correction for multiple comparisons.

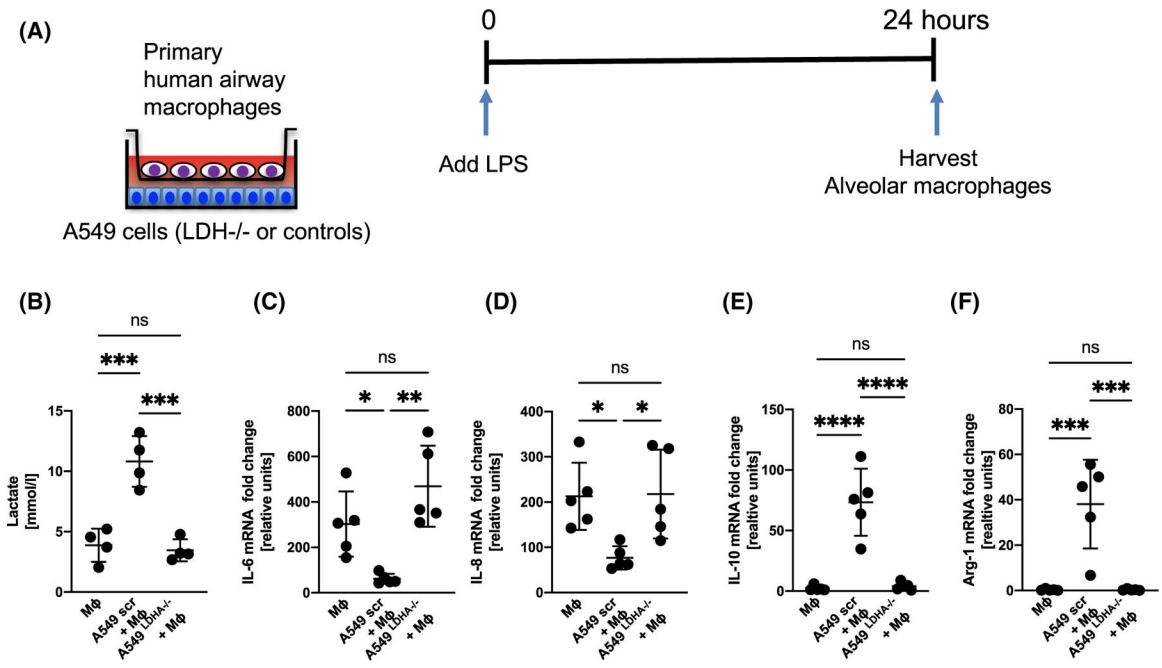

FIGURE 7.

Lactate produced by alveolar epithelial cells shifts primary human airway macrophage phenotype. Schematic of experiments (A). A549 cells (with stable knockdown of LDHA ($A549^{LDHA-/-}$ or scrambled controls (A549scr)) and primary human airway macrophages (MΦ) isolated from lungs rejected for donation were incubated in a non-contact insert co-culture system for 48 h prior to stimulation with 50 ng/mL LPS. Twenty-four hours after LPS stimulation, primary human airway macrophages were harvested and cytokines were measured with qPCR (A–F). $n = 5$/group. Data are represented as mean ± SD, ns = not significant, *$p < .05$, **$p < .01$, ***$p < .001$, ****$p < .0001$. Data were analyzed with one-way ANOVA with Tukey's correction for multiple comparisons.